Mathematical Model Of Turbulent Flow By SMAC Method Using Algebraic Stress Turbulence Model

Amir haghighatkhah
Master of Mechanical Engineering
Tehran, Iran
haghighatkhah.eng@gmail.com

Hossein Ahmadi-Danesh-Ashtiani
Islamic azad university, PhD ,Department of Mechanical Engineering, South Tehran Branch, Islamic Azad University, Tehran, Iran
h_a_danesh@azad.ac.ir
hdanesh1381@yahoo.com

Milad Abdollahi Kahriz
Tehran, Iran
Miladmak@yahoo.com

Kourosh Amiraslani,
Islamic azad university, PhD ,Department of Mechanical Engineering South Tehran Branch, Islamic Azad University, Tehran, Iran
k_amiraslani@azad.ac.ir

***Abstract*—The main purpose of this paper is to model the turbulent flow field and to determine the effect of using the k-ε turbulence model and the algebraic stress model (A.S.M) compared to the laminar model. To achieve this goal, the equations governing the turbulent flow in two-dimensional and non-continuous states are obtained, and in the next step, in order to complete the said equations, the A.S.M turbulence model is selected. In this research, the SMAC method is used, in which the nonlinear differential equations are discretized using the finite difference method, and the discrete equations are solved using the iterative method.**

The SMAC program, which is actually a simplified model of the MAC program, uses a combination of Illyrian and Lagrangian perspectives. In other words, this method uses Lagrangian particles that represent the fluid mass in the Eulerian lattice, which represents the solution. The most important disadvantage of the SMAC method is that it assumes that the flow is smooth and layered, and therefore in the present study to correct this defect, by modifying the existing k-ε turbulence model and also completing the program. The ASM turbulence model tries to show the effect of the turbulence model on the results.

Keywords*— *Mathematical modeling, SMAC method, Algebraic stress perturbation model, Algebraic perturbation models.

I. INTRODUCTION

With the increasing progress and increasing speed of computers, numerical methods have found a special place in solving computational fluid dynamics problems [1]. Given that the equations governing the turbulent flow field are nonlinear partial differential equations [2], to solve them, these partial differential equations must first be discretized and converted into algebraic equations, which for this purpose are often The finite difference method is used [3]. Then the generative algebraic equations are solved by direct solution method or iteration method [4]. Using the finite difference method, most of the dynamical problems of computational fluids such as unstable states can be solved [5]. For this purpose, Eulerian and Lagrangian views can be used. However, the use of combined Eulerian-Lagrangian methods gives better results [6]. In Euler's view, the focus is on a number of points in space and fluid changes are expressed as a function of time at these points, while in the Lagrangian method, the focus is on small fluid elements and changes in fluid elements to It is a function of time. In methods, fluid composition is considered as a number of Eulerian elements that are fixed in place and a set of Lagrangian particles is considered to show the movement of fluid through the network of elements. Flow variables such as velocity and pressure are assigned to points on the Eulerian lattice, and Lagrangian particles are used only to display fluid properties such as density.

The MAC program was one of the first programs to use the Euler-Lagrangian combination method [7] and later several researchers worked on improving this program, which resulted in the introduction of the SMAC program. The most important disadvantage of this program can be considered as a layer of flow. In other words, the effect of flow turbulence is not considered in this program [8]. Therefore, in the present study, we have tried to obtain a real analytical analysis of the turbulent flow in the governing equations by using a suitable turbulence model and considering the effect of Reynolds stresses. The method of work in the present study is that the turbulence of the flow is modeled using the algebraic stress model.

II. GOVERNING EQUATIONS

The continuity equation for turbulent flow is written as follows [9]:

$$\frac{\partial u_i}{\partial x_i} = 0 \quad (1)$$

Also, the momentum equation for turbulent flow is written as follows [9]:

$$\frac{\partial u_i}{\partial t} + u_j \frac{\partial u_i}{\partial x_j} = -\frac{1}{\rho_r}\frac{\partial P}{\partial x_i} + \frac{\partial}{\partial x_j}\left(v\frac{\partial u_i}{\partial x_j} - u_i u_j\right) + g_i \frac{\rho-\rho_r}{\rho_r} \quad (2)$$

In the above relations, u_i represents the instantaneous velocity component in the x_i direction, and v represents the molecular viscosity, ρ_r the reference density, ρ the local density, and finally g_i the gravitational acceleration. It should be noted that the system of the above equations is not closed because there are nonlinear terms in which the process of averaging on them creates new relationships between velocity fluctuations, $u_i' u_j'$ [10].

The term $-\rho u_i' u_j'$ represents the momentum transfer of x_i in the x_j direction or vice versa. Due to the fact that this effect acts like a stress on the fluid, it is called Reynolds stress or turbulence [11]. In order to be able to solve Equations (1) and (2) for the mean values of velocity and pressure, the terms u_i' and u_j' must be specified [12]. In fact, the main problem in calculating turbulent flows is the determination of dependency terms [13]. True transfer equations can be obtained for $u_i' u_j'$ in different directions, but these equations also include higher degree dependence terms [14].

III. ALGEBRAIC STRESS MODEL (ASM)

In general, for three-dimensional currents, there are six Reynolds stress components. The model of complete turbulence is a model that has introduced the transfer equation for each of the stresses. Considering the equations k and ε and the Reynolds equations, the flow equation system includes 11 differential equations. In this case, the best technique is to simplify the equations by substituting algebraic expressions instead of partial differential terms.

The basic equation of transfer $u_i u_j$ is as follows.

$$\frac{D(u_i u_j)}{Dt} = Diffu_i u_j + P_{ij} + \emptyset_{ij} + D_{ij} \quad (3)$$

In the above relation $\frac{D(u_i u_j)}{Dt}$ is the substitute for the displacement transfer $u_i u_j$ by motion and $Diffu_i u_j$ is the substitute for the diffusion transfer by motion. P_{ij}, $\emptyset_{ij}$ and D_{ij} also represent production, strain-pressure and viscosity loss, respectively.

The gradients of the dependent variables in the transfer equations appear only in the rate of change, transfer, and propagation rates. Hence, if these sentences can be eliminated using relatively accurate approximations, the differential equation becomes an algebraic expression. The algebraic expression for $u_i u_j$ can be written as follows:

$$\frac{D(u_i u_j)}{Dt} - Diffu_i u_j = \frac{u_i u_j}{k}\left(\frac{Dk}{Dt} - Diffk\right) = \frac{u_i u_j}{k}(Pk - \varepsilon) \quad (4)$$

By placing the above relation in the transfer equation $u_i u_j$, the following relation is obtained for single stresses:

$$\frac{V'^2}{k} = \frac{2}{3}\frac{1-\left(\frac{P_k}{\varepsilon}\right)\emptyset_2}{1+2\emptyset_5} \quad (5)$$

$$\frac{u'^2}{k} = \frac{2}{3}\left(1 + \left(\frac{P_k}{\varepsilon}\right)\emptyset_4\right) + \emptyset_5 \frac{V'^2}{k} \quad (6)$$

$$u'v' = -\emptyset_1 \frac{V'^2}{k}\frac{k^2}{\varepsilon}\frac{\partial u}{\partial y} \quad (7)$$

In the above relations:

$$\emptyset_1 = \frac{(1-c_2+1.5c_2c_2'f)}{(\beta+1.5c_1'f)} \quad (8)$$

$$\emptyset_2 = \frac{(1-c_2'+2c_2'c_2f)}{(\beta)} \quad (9)$$

$$\emptyset_3 = \frac{(1-c_2+c_2c_2'f)}{(\beta)} \quad (10)$$

$$\emptyset_4 = \frac{(2-2c_2+c_2c_2'f)}{(\beta)}. \emptyset_5 = c_1' \frac{f}{\beta} \quad (11)$$

$$f = \frac{k^{\frac{3}{2}}C_\mu^{\frac{3}{4}}}{\varepsilon yk} \quad (12)$$

$$\beta = c_1 + \left(\frac{P_k}{\varepsilon}\right) - 1 \quad (13)$$

$$P_k = -u'v'\left(\frac{\partial u}{\partial y}\right) \quad (14)$$

$$C_\mu = \emptyset_1 \frac{v'^2}{k}, (c_1 = 1.8, c_2 = 0.6, c_1' = 0.5, c_2' = 0.3) \quad (15)$$

IV. FINITE DIFFERENCE EQUATIONS

In the SMAC method, Reynolds equations are discretized using the FTCS method. In this method, the forward difference method is used for the time derivative and the central difference method is used for the spatial derivative.

For example, the Reynolds equation is discretized in the x direction around the point (i + 1/2, j) as follows:

Journal of Multidisciplinary Engineering Science and Technology (JMEST)
ISSN: 2458-9403
Vol. 9 Issue 5, May - 2022

$$\frac{1}{\delta t}\left(u_{i+\frac{1}{2}j}^{n+1} - u_{i+\frac{1}{2}j}\right) = \frac{1}{\delta x}\left(u_{i+\frac{1}{2}j}.u_{i-\frac{1}{2}j} - u_{i+\frac{3}{2}j}.u_{i+\frac{1}{2}j}\right) + \frac{1}{\delta y}\left[(uv)_{i+\frac{1}{2}j-\frac{1}{2}} - (uv)_{i+\frac{1}{2}j+\frac{1}{2}}\right] - \frac{1}{\delta x}\left(\theta_{i+ij} - \theta_{i,j}\right) + g_x + v\left[\frac{1}{\delta y^2}\left(u_{i+\frac{1}{2}j+1} + u_{i+\frac{1}{2}j-1} - 2u_{i+\frac{1}{2}j}\right) - \frac{1}{\delta x\delta y}\left(v_{i+j+\frac{1}{2}} - v_{i,j-\frac{1}{2}} - v_{i,j+\frac{1}{2}} + v_{i,j-\frac{1}{2}}\right)\right] - \frac{1}{2\delta x}\left(u'^2_{i+\frac{3}{2j}} - u'^2_{i-\frac{1}{2j}}\right) + \frac{1}{\delta y}\left(v_{tij+1} - v_{ti+1,j}\right).\frac{1}{\delta y^2}\left(u_{i+\frac{1}{2}j+1} + u_{i+\frac{1}{2}j-1} - 2u_{i+\frac{1}{2}j}\right)$$
(16)

To discretize the equations k and ε depending on the value of the Reynolds number of the grid, the type of discretization will be different. The network Reynolds number indicates the transmission power relative to the transmission power in a transmission-distribution equation. For governing equations, this number is defined as x and y:

$$Re_x = \frac{u\delta x}{v_t}, \quad Re_y = \frac{u\delta y}{v_t}$$
(17)

The FTUS method is used when the network Reynolds number is greater than 2 and the FTCS method is used when the network Reynolds number is less than or equal to 2.

The subtitle ij corresponds to the position of the element within the Eulerian network, and the uppercase n + 1 indicates the quantity at time t = (n + 1) δt. All quantities are without balances for time n. As shown in Figure (1), the variables θ, Ψ, k and ε are in the center of the element and the velocity components u and v are on the element faces.

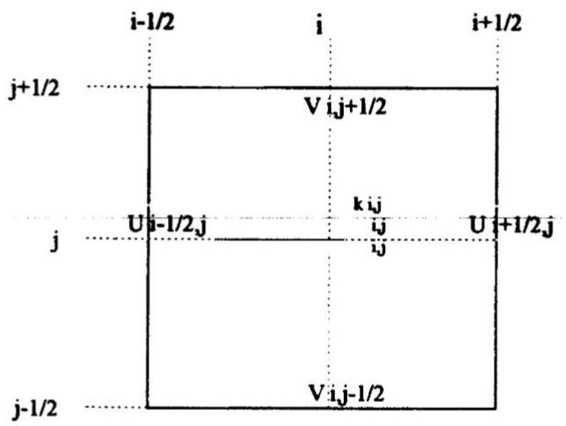

figure 1. Position of flow variables in the element

V. Solving steps

In the first step, the initial velocity fields are calculated using the provided relations. In this step, each pressure field can be selected optionally, but in order to increase efficiency and speed, the hydrostatic pressure distribution is used as follows.

θ_ij= g_x x_i+ g_y y_j
(18)

For free surface elements of the fluid, the value of θ is equal to the vertical stresses plus the applied surface pressure. In this step, all velocities perpendicular to the rigid walls are considered zero. Also, velocity is not calculated on the empty face of surface elements. The value of velocity on this aspect is calculated in the third step based on satisfying the continuity condition.

In the second step, the initial speeds are converted to the final speeds. This is done using the pressure potential function gradient (Ψ) as follows:

u_(i+1/2 j)^(n+1)= u ̃_(i+1/2 j)^(n+1)-1/δx (Ψ_(i+1,j)-Ψ_(i,j))
(19)

V_(i+1/2 j)^(n+1)= V ̃_(i+1/2 j)^(n+1)-1/δy (Ψ_(i+1,j)-Ψ_(i,j))
(20)

In the last step, the velocities obtained in the second step are used to move the Lagrangian particle set. These particles merely express the state of the fluid mass and its free surface.

A free-slip boundary represents an axis of symmetry or a friction-free surface that exerts no shear stress on the fluid. The velocity component perpendicular to the wall is zero. The components of tangential velocity, potential function, kinetic energy of compression and energy loss without gradient are considered:

u_(i-1/2,j)=0, Ψ_(i-1,j)= Ψ_(i,j), v_(i-1/2,j+1/2)=v_(i.j-1/2), k_(i-1,j)= k_(i,j), v_(i-1/2,j-1/2)= v_(i,j-1/2), ε_(i-1,j)=ε_(i,j)
(21)

A non-slip boundary represents an adhesive boundary that exerts a shear stress on the fluid. The tangential velocity component on this boundary is zero.

u_(i-1/2,j)=0, Ψ_(i-1,j)= Ψ_(i,j), v_(i-1,j+1/2)= 〖-v〗_(i.j-1/2), k_(i-1,j)= k_(i,j), v_(i-1,j-1/2)= v_(i,j-1/2), ε_(i,j)=(u_(i+1/2,j)^*)^3/0.2δx, k_(i,j)= (u_(i+1/2 j)^*)^2/(cμ^0.5)
(22)

VI. Results

Solving equations using the finite difference method is associated with several errors that due to the existence of these errors, the calculated results differ from the actual results. The value of this difference is directly a function of the numerical method and the type of discretization used. In this research, we have tried to use the most appropriate method to reduce errors as much as possible. In this article, we have tried to use the most appropriate method to reduce errors as much as possible. The process of determining the type of discretization in the program is such that in the first step, the equations are discretized using the FTUS method, which in practice due to the existence of a numerical distribution that is due to the cut-off error, in practice none of the models converge. And does not lead to a definite result, of course, by considering the dimensions of the network smaller, the amount of numerical distribution can be reduced and the calculation error can be reduced, but in this case, the value of δt must be considered very small, which causes Increases the calculation time. Also, due to the limited memory of the device, the number of elements is limited in selection, and due to the very small Δx and Δy, the dimensions of the flow field are very small, which will not have a physical interpretation.

If the central difference method is used in discretization, it causes unrealistic fluctuations in the response. Therefore, in discretizing the equations, a combined method consisting of Upwind and Central methods is used.

In this research, the presented models have been implemented on two different options. Considering that the main purpose of this paper was to use different turbulence models on the flow field, the quiet, k-ε and ASM models were implemented on one option and the results were compared and the results of the mentioned models on another option. Has also been calculated and compared with existing laboratory and numerical data.

In general, in this research, two types of sedimentation ponds have been considered, in which the location of the inlet flow is different and the outflow of the flow has been done from the overflow head. In the first case, where the results obtained from the SMAC method are compared with the k-ε and A.S.M models, the location of the inlet flow is from the floor and the height of the inlet flow is half the depth of the flow in the pond. The geometric characteristics of this pond are given in Figure (2) and Table (1).

Table 1. Dimensions and hydraulic characteristics of the first geometry

$\Delta x(m)$	$\Delta y(m)$	L (m)	$h_1(m)$	$h_2(m)$	h (m)	Fr
0.1	0.02	1.0	0.08	0.08	0.16	0.56

The results of model implementation for the first geometry are given in Figures (3) to (5). These diagrams show the velocity profile along the pond, the velocity vector in the solution field, as well as the flow lines due to the model run.

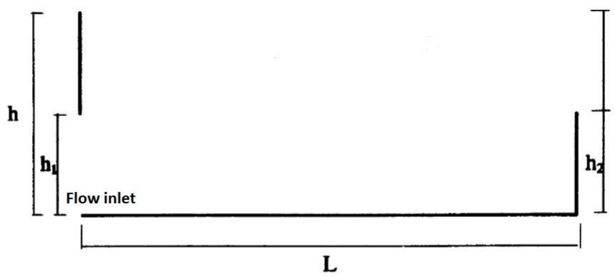

figure 2. Geometric and hydraulic characteristics of the first geometry

In the laminar flow model, the viscosity is 10,000 times that of the actual viscosity, but it can be seen that in practice this model can not predict the effect of turbulence on the flow field. In Figures (4) and (5) it is clear that the turbulence in the A.S.M model is greater than k-ε and also in this case a rotational region is formed that the length of this region is somewhat different in the two mentioned countries.

During the implementation of the program for different inlet conditions, it was found that in a field with a known depth of field, the smaller the ratio of the inlet flow depth to the total flow depth, the more intense the rotational zone is created, which will definitely have a greater effect on the flow pool. For the first geometry, where the flow inlet from the bottom of the pond is considered, the length of the rotational zone in the A.S.M model is 3 times the flow depth and in the k-ε model is about 2.7 times the flow depth.

Figures (6) to (8) also show the velocity vectors for the computational field for the three modes of slow flow, the k-ε turbulence model and the A.S.M turbulence model. Figures (9) to (11) show the flow lines for the turbulence models, respectively.

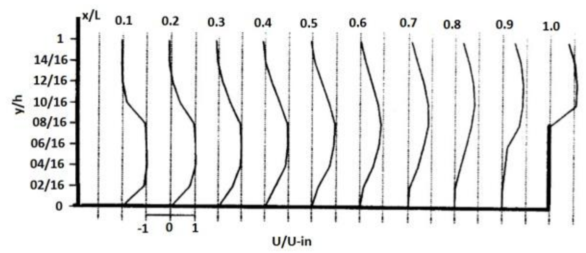

Figure 3. Horizontal velocity profiles in the pond for smooth flow and first geometry

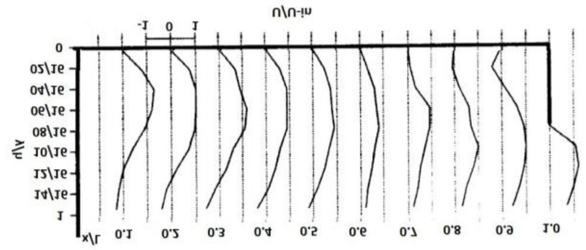

Figure 4. Horizontal velocity profiles in the pond for turbulent flow with model k-ε and first geometry

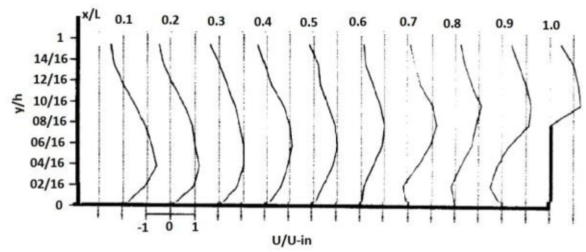

Figure 5. Horizontal velocity profiles in the pond for turbulent flow with the A.S.M model and the first geometry

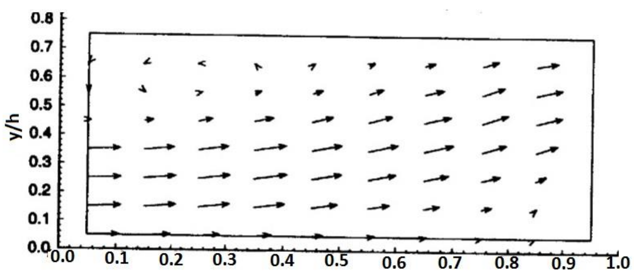

Figure 6. Velocity vector profiles in the pond for smooth flow and first geometry

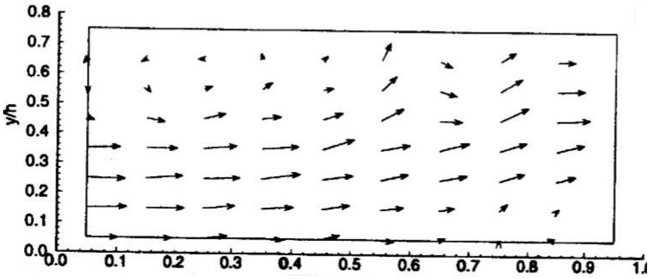

Figure 7. Velocity vector profiles in the pond for turbulent flow with model k-ε and first geometry

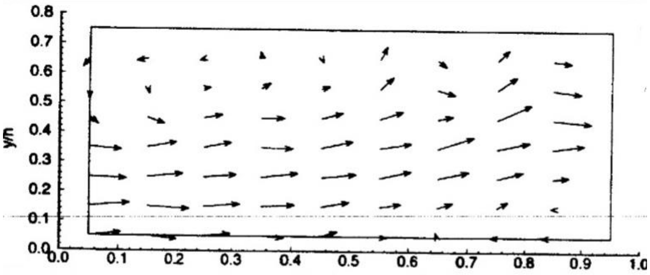

Figure 8. Velocity vector profiles in the pond for turbulent flow with the A.S.M model and the first geometry

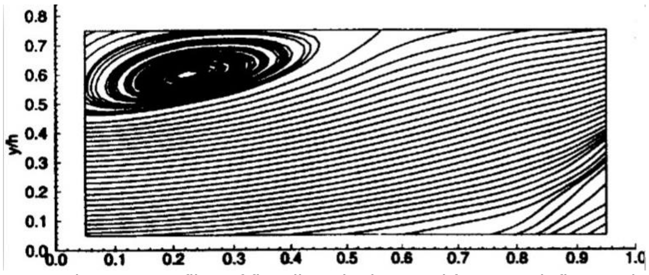

Figure 9. Profiles of flow lines in the pond for smooth flow and first geometry

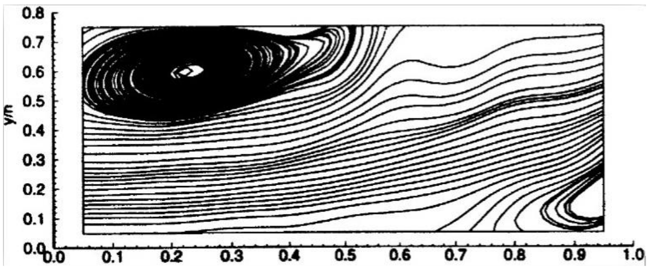

Figure 10. Profiles of flow lines in the pond for turbulent flow with model k-ε and first geometry

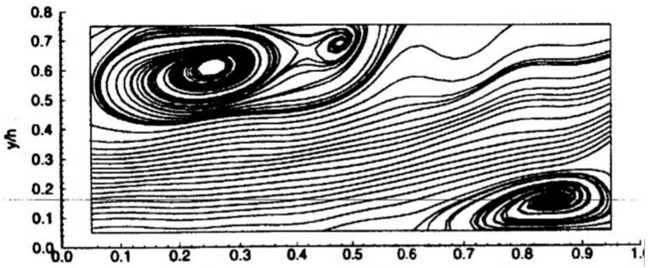

Figure 11. Profiles of flow lines in the pond for turbulent flow with A.S.M model and first geometry

VII. CONCLUSION

In this study, with the aim of simulating turbulent flow, the governing Reynolds equations have been solved using k-ε and A.S.M turbulence models. The governing equations are discretized using the finite difference method. The use of the A.S.M model has been shown to better predict eddy currents than the k-ε model.

References

[1] Harish, R. (2018). Buoyancy driven turbulent plume induced by protruding heat source in vented enclosure. International Journal of Mechanical Sciences, 148, 209-222.

[2] Harish, R. (2018). Effect of heat source aspect ratio on turbulent thermal stratification in a naturally ventilated enclosure. Building and Environment, 143, 473-486.

[3] Waman, W., & Harish, R. (2020). Influence of volume blockage ratio on turbulent buoyant plume dispersion in mixed ventilated tunnel. Journal of Wind Engineering and Industrial Aerodynamics, 207, 104397.

[4] List, B., Chen, L. W., & Thuerey, N. (2022). Learned Turbulence Modelling with Differentiable Fluid Solvers. arXiv preprint arXiv:2202.06988.

[5] Shah, N., Dwivedi, V., & Sedani, B. (2019, December). Comparative Analysis of Relay Selection Techniques in Free Space Optics. In 2019 Third International conference on I-SMAC (IoT in Social, Mobile, Analytics and Cloud)(I-SMAC) (pp. 547-550). IEEE.

[6] Harish, R., & Sivakumar, R. (2021). Effects of nanoparticle dispersion on turbulent mixed convection flows in cubical enclosure considering Brownian motion and thermophoresis. Powder Technology, 378, 303-316.

[7] Adamczewski, P. (2018). Knowledge management of intelligent organizations in turbulent environment. Economic and Social Development: Book of Proceedings, 413-422.

[8] Harish, R., & Sivakumar, R. (2021). Turbulent thermal convection of nanofluids in cubical enclosure using two-phase mixture model. International Journal of Mechanical Sciences, 190, 106033.

[9] Kim, J. (2019). Evaluation of RANS k–ε calculations for turbulent stably stratified layers based on GEMIX experiments using the CUPID code. International Communications in Heat and Mass Transfer, 108, 104341.

[10] Rezaei, H., & Ketabdari, M. J. (2022). A two-phase flow numerical modeling of plunging breaking solitary waves using artificial slope variation. Journal of Ocean Engineering and Science.

[11] Booshi, S., & Ketabdari, M. J. (2021). Modeling of solitary wave interaction with emerged porous breakwater using PLIC-VOF method. Ocean Engineering, 241, 110041.

[12] Suga, K., Sakamoto, T., & Kuwata, Y. (2019). Algebraic non-equilibrium wall-stress modeling for large eddy simulation based on analytical integration

of the thin boundary-layer equation. Physics of Fluids, 31(7), 075109.

[13] Wang, H., Wang, H., Gao, F., Zhou, P., & Zhai, Z. J. (2018). Literature review on pressure–velocity decoupling algorithms applied to built-environment CFD simulation. Building and Environment, 143, 671-678.

[14] Biannic, J. M., & Roos, C. (2018). Robust Autoland Design by Multi-Model $\mathcal{H}\infty$ Synthesis with a Focus on the Flare Phase. Aerospace, 5(1), 18.